Noname manuscript No.
(will be inserted by the editor)

Analysis of Nominal Halo Orbits in the Sun–Earth System

Elbaz I. Abouelmagd · Juan Luis García Guirao · Ashok Kumar Pal

Received: date / Accepted: date

Abstract In this paper, the effect of radiation pressure force on formation of the nominal halo orbit around the collinear point L_1 is estimated. It is developed in the framework of Sun–Earth system. In the third–order approximation, using Lindstedt–Poincaré technique, the radiation pressure effect on nominal halo orbits is computed. Further, we develop the solution into a Fourier series of nominal halo orbit. According to the radiation pressure force, the analysis can be used to design trajectory for spacecraft traveling in more realistic system.

Keywords Restricted three–body problem · Radiation pressure · Halo orbit · Fourier series.

1 Introduction

The three–body problem is one of the most dynamical systems which have been repeatedly and deliberated studied in celestial mechanics. Of specific interest are the infinitesimal body trajectory motion under the gravitational effect of the other two finite bodies. Recently these systems have been received considerable numerical and analytical analysis [1–7]. In general the restricted three–body problem has five libration points. Two of them are called triangular points, L_4 and L_5, while the other are called collinear points, L_1, L_2 and L_3, which take locations on the joining line between the primaries [8–13].

The libration points in the Earth–Moon or Sun–Earth systems are equilibrium points in the gravitational field, where the spacecrafts can preserve stationary without consumption of extra–fuel [14, 15]. The dynamics around libration points furnishes periodic orbits families. Which are serviceable for placing a spacecraft and has an extraordinary advantageous for solar observation and astrophysics missions as well as communication links etc. [16]. In fact, these points have a considerable significance in the Sun–Earth system. In particularly, the point L_2, which lies between the Sun and Earth. Because it has a unrivaled feature in the activity of solar observation due to its unique location. Therefore, the libration points missions are of exceptional interest in the recent time [16].

A halo orbit is a three dimensional periodic orbit near the libration points L_1, L_2 and L_3, in the restricted three–body problem [17, 18]. A survey on the used methods, which depend on the Hamiltonian dynamical systems properties within frame of three or more degrees of freedom, to purpose of spacecrafts missions in the proximity of collinear libration points have been presented [19]. Also they used a combination between symbolic and numerical methods to design the nominal orbit. Further, the local investigations of the dynamics around this orbit are performed for station–keeping and transfer manoeuvres.

Halo orbits will generate as resulting from the mutual interaction among the gravitational pull of two planetary bodies, the coriolis and centrifugal acceleration on an infinitesimal body or spacecraft. We can find these orbits in any three–body system, for example [20, 21], but not limited to the Sun–Earth–Orbiting Spacecraft or Satellite systems or the Earth–Moon–Orbiting Spacecraft or Satellite systems. Although, the families of southern and northern halo

Elbaz I. Abouelmagd
Celestial Mechanics and Space Dynamics Research Group (CMSDRG), Astronomy Department,
National Research Institute of Astronomy and Geophysics–NRIAG, 11421–Helwan, Cairo, Egypt eabouelmagd@gmail.com or elbaz.abouelmagd@nriag.sci.eg.

Juan Luis García Guirao
Departamento de Matemática Aplicada y Estadística. Universidad Politécnica de Cartagena,
Hospital de Marina, 30203-Cartagena, Región de Murcia, Spain.
juan.garcia@upct.es

Ashok Kumar Pal (✉)
Department of Mathematics and Statistics, Manipal University Jaipur,
Jaipur-303007, Rajasthan India.
ashokpalism@gmail.com

orbits are existing at each collinear libration points, but these orbits tend to be unstable, so the station–keeping is desired, to conserve a spacecraft on the orbit [22–24]

In the last decades, there are many works have been addressed to investigate the dynamic of halo orbits around the collinear libration points. The strategy of transfer from the proximity of the Earth to halo orbits around the equilibrium collinear point between the Sun and Earth have been studied by [25]. The quasibicircular model of Earth–Moon–Sun–Spacecraft case is considered, which is more coherent model than the restricted three–body problem (RTBP), to compute the quasiperiodic translunar Halo orbits. These orbits are determined with using a continuation method starting at the RTBP halo orbits [26].

Recently, [27] have developed numerical method to analyze the Halo/Lissajous orbits in the proximity of libration collinear points in the frame work of a full solar system model. They have proposed a full solar system gravitational model, in the synodic coordinate frame with an explicit investigation for the angular velocity with respect to the inertial reference frame. Based on a dynamical analysis of the Poincaré surfaces sections, an alternative technique to find the patch points in the multiple shooting method is addressed. Furthermore, by depending on the new patch points and sequential quadratic programming. They have developed halo orbits around the libration points L_1, L_2, and L_3, while Lissajous orbits are developed around L_1, L_2, points in the Earth–Moon system, with the proposed full gravitational solar system model to verify the impact of used method.

There are many considerable projects proposed by the major space agencies. Some of these projects are Deep Space Climate Observatory (DSCOVR), National Aeronautics and Space Administration (NASA), LISA Pathfinder which is an ESA (European Space Agency) mission and Spektr–RG (Roscosmos/ESA), see for more details [22]. The collinear libration points of the Sun–Earth system are used in most of these projects. But the same associated points in the Earth–Moon system have attracted an extra attention, in particularly, after the success of the ARTEMIS missions to the Earth–Moon collinear equilibrium points [28, 29]. The ARTEMIS mission is performed to study the Earth's magnetotail regions. This mission is considered one of the most familiar missions to Earth–Moon collinear libration points.

There are also some significant applications to collinear points missions including communications, surveillance, observation, space navigation and human operations etc. But the most of these missions concentrated on impulsive transfers to libration points. The optimization of a low-thrust transmit from the Earth orbit to the halo orbit around the libration points between the Earth and Moon has been investigated [30]. They also used Particle Swarm Optimization (PSO) for pruning the search space of a low-thrust path transmit from the Earth orbit to a libration point orbit in the Earth-Moon system. In this context, the choice of a nominal space telescope orbit around libration point within frame of the Sun–Venus system (the point from only the Venus side) is analyzed from the illumination viewpoint conditions and station–keeping costs [24]. Some more studies for geostationary orbits using hybrid low-thrust propulsion and solar sail are described [31, 32].

[33] have studied the effect of oblate and prolate of magnetic planet on equatorial and halo orbits. While in this paper, we examine the effect of radiation pressure force on formulation of halo orbit around collinear point L_1 in the Sun-Earth-infinitesimal mass circular restricted three-body system using the Lindstedt–Poincaré method. Further, we express the solution as in the form of Fourier series.

This paper is organized as follows. In Section 2, we recall the equations of motion of the circular restricted three-body problem with radiation pressure force around the libration point L_1. In Section 3, we describe the periodic motion in the proximity of the libration point L_1 and using the Lindstedt–Poincaré technique to compute the halo orbit. In Section 4, we analyze the solution correction in out–of–plane motion. In Section 5, we expand the third order analytical solution in Fourier series and the coefficients are found by Simpson's composite method. Finally the conclusions have been given in Section 6. At the end, we write the Appendix A.

2 Formulation of the model

Equations of motion for an infinitesimal body moving in vicinity of the collinear point L_1 in the Sun-Earth circular restricted three–body system, obtain from the equations of motion of the photogravitational circular restricted three-body problem [34]. In order to find the halo orbit around L_1 point, the origin of the reference system will be shifted to the location of the collinear point L_1 and scaled by $\xi = -\gamma(1-x) + \mu - 1$, $\eta = -\gamma y$ and $\zeta = \gamma z$. Hence, the full three–dimensional equations of motion with radiation pressure force are given as [35]

$$\begin{aligned} x'' - 2y' - (1+2c_2)x &= S_x, \\ y'' + 2x' + (c_2 - 1)y &= S_y, \\ z'' + c_2 z &= S_z, \end{aligned} \tag{1}$$

where

$$S_x = \frac{\partial}{\partial x}\sum_{n\geq 3} c_n \rho^n P_n\left(\frac{x}{\rho}\right),$$
$$S_y = \frac{\partial}{\partial y}\sum_{n\geq 3} c_n \rho^n P_n\left(\frac{x}{\rho}\right),$$
$$S_z = \frac{\partial}{\partial z}\sum_{n\geq 3} c_n \rho^n P_n\left(\frac{x}{\rho}\right),$$

here $P_n(\varphi)$ is the Legendre polynomial of order n with respect to the variable φ, and the constant c_n $(n = 0, 1, 2, ...)$ is given by

$$c_n = \frac{1}{\gamma_L^3}\left[\mu + (-1)^n \frac{(1-\beta)(1-\mu)\gamma^{n+1}}{(1-\gamma)^{n+1}}\right].$$

While a dimensionless quantity β is introduced [36]to specify the effect of radiation pressure and P-R drag. It is defined as ratio of the radiation pressure force to the solar gravitation force.

With some simple calculations Eq. (1) can be rewritten in following form

$$\begin{aligned} x'' - 2y' - (1+2c_2)x &= S_1, \\ y'' + 2x' + (c_2 - 1)y &= S_2, \\ z'' + c_2 z &= S_3, \end{aligned} \tag{2}$$

where

$$S_1 = \sum_{n\geq 2}(n+1)c_{n+1}\rho^n P_n\left(\frac{x}{\rho}\right),$$
$$S_2 = \sum_{n\geq 3} c_n y \rho^{n-2}\bar{P}_n\left(\frac{x}{\rho}\right),$$
$$S_3 = \sum_{n\geq 3} c_n z \rho^{n-2}\bar{P}_n\left(\frac{x}{\rho}\right),$$

and the quantity $\bar{P}_n(x/\rho)$ denotes

$$\bar{P}_n\left(\frac{x}{\rho}\right) = \sum_{k=0}(3+4k-2n)P_{n-2k-2}\left(\frac{x}{\rho}\right).$$

Units are defined as sum of the mass of the Sun and Earth is unit, distance between the Sun and Earth is unit and the unit of time is defined as the time period of the rotating frame. Further, we take μ is the unitless mass of the Earth, γ is the dimensionless quantity defined as the distance between collinear point L_1 to the Earth and $\rho^2 = x^2 + y^2 + z^2$.

3 Solutions and manifolds

In case of neglecting the second and higher order terms of space variable x, y and z, then the left hand side of Eqs (2) represent the equations of linearized system. Hence the first two equations are coupled and admit the planar motion in xy–plane, while the third equation represents the out–of–plane motion in the form of a simple harmonic motion. Thereby, the characteristic equation of the planar system will yield two real and imaginary roots which are called $\pm\alpha$ and $\pm i\lambda$.

$$\alpha = \sqrt{\frac{c_2 - 2 + \sqrt{9c_2^2 - 8c_2}}{2}},$$
$$\lambda = \sqrt{-\frac{c_2 - 2 - \sqrt{9c_2^2 - 8c_2}}{2}},$$

and the out-of-plane motion will yield two imaginary roots, say $\nu = \pm i\sqrt{c_2}$. These roots give nature of the orbits which are perturbing by the radiation pressure effect.

In the range of approximately $\beta \in [0,\ 0.04]$, the roots are decreasing and further they increase with exponential rate as $\beta \to 1$. In Fig. 1, β has approximately same affect on λ (blue curve) and ν (red curve), whereas on the α (black curve) has the high rate of influence by the parameter β. Moreover, the sign of these roots are not changed due to introducing the β, therefore, it does not affect the stability. The libration points are unstable as well. Hence, the manifolds associated to these points are unstable or have unstable parts, then it needs station-keeping.

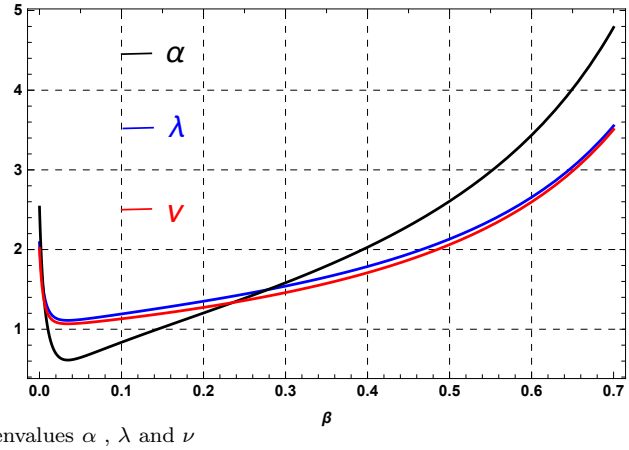

Fig. 1 The effect of β on the eigenvalues α , λ and ν

In this way, the general solutions of the linear system are given by

$$\begin{aligned} x &= A_u e^{\alpha t} + A_s e^{-\alpha t} - A_x \cos(\lambda t + \phi), \\ y &= \kappa_1 A_u e^{\alpha t} + \kappa_1 A_s e^{-\alpha t} + \kappa A_x \sin(\lambda t + \phi), \\ z &= A_z \sin(\nu t + \psi), \end{aligned} \tag{3}$$

for a certain epoch t, we compute position and velocity of the infinitesimal body in terms of the amplitudes and phases. But the Eqs. (3) represent a solution of quasi–periodic motion for the linearized system. Thereby the improper choice of the initial conditions will yield unbounded motion with growing time. For bounded and periodic motion, the choice of the arbitrary conditions will be restricted to set $A_u = A_s = 0$. In this case we will obtain the Lissajous orbits where A_x and A_z are amplitude of motions, while ϕ and ψ are different phases in–plane and out–plane respectively. Furthermore, for stable (unstable) manifold, we set $A_u = 0$ and $A_s \neq 0$ ($A_s = 0, \quad A_u \neq 0$) and for square Lissajous orbit around L_1 point, we characterized $A_x = A_z$. Moreover, the solution of linearized equations of above system is unbounded. However, if the initial conditions are restricted and only the non–divergent mode is allowed, then solution can be expressed in the following form

$$\begin{aligned} x &= -A_x \cos(\lambda t + \phi), \\ y &= k A_x \sin(\lambda t + \phi), \\ z &= A_z \sin(\nu t + \psi), \end{aligned} \tag{4}$$

here λ and ν are in–plane and out–of–plane motions frequencies.

In general, the in–plane and out–of–plane frequencies λ and ν are unequal. So that the three dimensional linearized motion will be quasi–periodic. The projections of the motion on the different plane produce the Lissajous–type trajectories.

The linearized equations as an intermediate Lissajous orbit, on which to build higher–order successive approximations corrections would be unacceptable [37]. If the amplitude of in–plane and out-of-plane motions are of sufficient magnitude and so the non–linear contribution to the system produce equal eigenfrequencies and replacing ν by λ. Hence Eqs. (4)will be rewritten in the below form

$$\begin{aligned} x &= -A_x \cos(\lambda t + \phi), \\ y &= \kappa A_x \sin(\lambda t + \phi), \\ z &= A_z \sin(\lambda t + \phi). \end{aligned} \tag{5}$$

By aforementioned condition, the periodic solutions are called halo orbit solutions. Hence the above solutions (5) represent periodic orbits, which are called the halo–type solutions.

4 Solution Correction in out–of– plane motion

The used approximations to find the halo–type solutions are not concern to the linearized system only, but also these approximations include that the frequencies of the in–plane and out–of plane are equal. Therefore, it becomes mandatary to insert a correction term Δ, where $\Delta = \lambda^2 - c_2$. The quantity Δ is a significant constraints for frequency correction and also affected by the parameter of radiation pressure β. This influence is shown in Fig. 2. It decreases in $[0,\ 0.03]$ and further increases exponentially.

Nature of the parameter c_2, α, λ, Δ, and κ are perturbed because of the radiation pressure. They are decreasing very fast in the interval $\beta \in [0,\ 0.1]$, which shown in Table 1 and it increases exponentially as $\beta \to 1$.

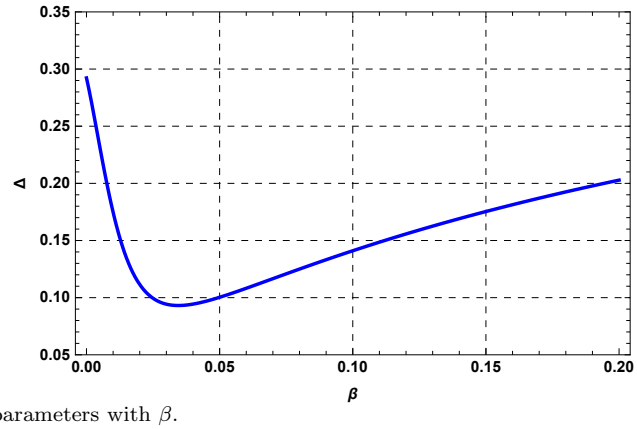

Fig. 2 The effect of β on Δ.

Table 1 Effective change in all parameters with β.

β	c_2	α	λ	Δ	κ
0.0	4.06107	2.53266	2.08645	0.292214	3.22927
0.1	1.27898	0.83606	1.19165	0.141042	2.08870
0.2	1.62298	1.20365	1.35122	0.202809	2.24677
0.3	2.13103	1.58303	1.54108	0.243914	2.47780
0.4	2.92161	2.02886	1.78736	0.273039	2.80802
0.5	4.25019	2.60665	2.13177	0.294272	3.29417
0.6	6.74367	3.43469	2.65583	0.309786	4.05537
0.7	12.3017	4.78793	3.55282	0.320835	5.37966
0.8	29.1626	7.52684	5.43054	0.328174	8.17745
0.9	137.211	16.5153	11.7279	0.332250	17.6062

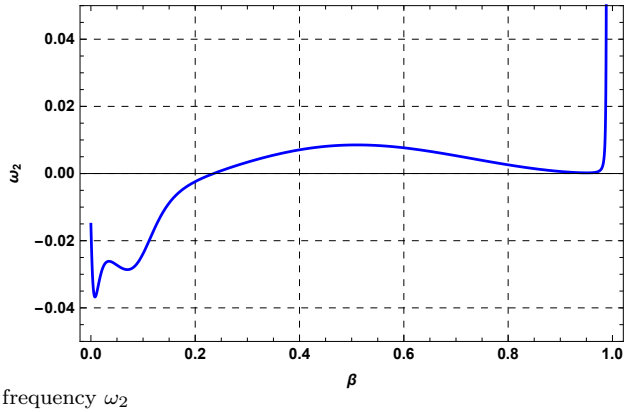

Fig. 3 The effect of the β on the frequency ω_2

Using the correction term Δ, we rewrite the third equation of Eq. (2) as

$$z'' + \lambda^2 z = \sum_{n\geq 3} c_n z \rho^{n-2} \bar{P}_n \left(\frac{x}{\rho}\right) + \Delta z.$$

Using the Lindstedt–Poincaré technique we introduce an independent variable $\tau = \omega t$ to remove the secular terms. Therefore, the frequency correction ω is defined as

$$\omega = 1 + \sum_{n\geq 1} \omega_n, \tag{6}$$

where $\omega_n < 1$.

Accordingly to develop the third–order periodic solution and remove the secular terms as [18, 38], it is found that $\omega_1 = 0$, and $\omega_2 = s_1 A_x^2 + s_2 A_z^2$,

were s_1 and s_2 are described in Appendix A. When the radiation pressure force increases, the quantity ω_2 changes its nature as shown in Fig. 3. While the time-period of the nominal halo orbit fluctuates with increasing the value of the β, shown in Fig. 4.

The amplitude relation is obtained using the expression ω_2 and the constraints which obtain after removing the secular terms. It is written as

$$l_1 A_x^2 + l_2 A_z^2 + \Delta = 0 \tag{7}$$

where the coefficients l_1 and l_2 are defined in the Appendix A. Further, values of the parameters on the different value of β are described in Table 2.

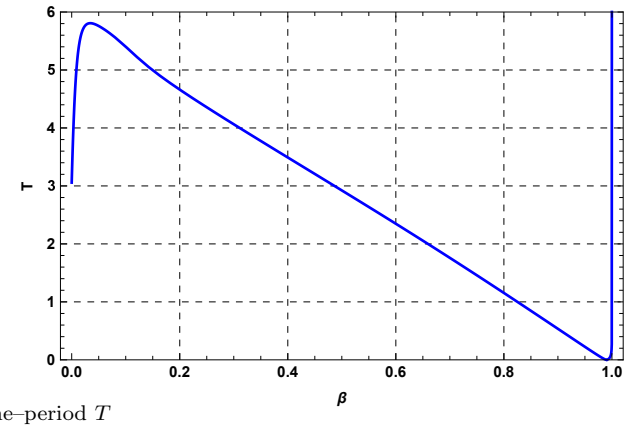

Fig. 4 The effect of β on the time–period T

Table 2 β on A_x, ω_2 and Time-period T

β	A_x	ω_2	T
0.0	± 0.1352880	− 0.01509350	3.05757
0.1	± 1.9043800	− 0.02386990	5.40163
0.2	± 1.2774300	− 0.00240244	4.66122
0.3	± 0.6239050	0.00337724	4.06340
0.4	± 0.3063230	0.00706592	3.49068
0.5	± 0.1433380	0.00850835	2.92253
0.6	± 0.0604325	0.00766398	2.34781
0.7	± 0.0211072	0.00530589	1.75917
0.8	± 0.0050856	0.00259265	1.15402
0.9	± 0.0004546	0.00061298	0.53542

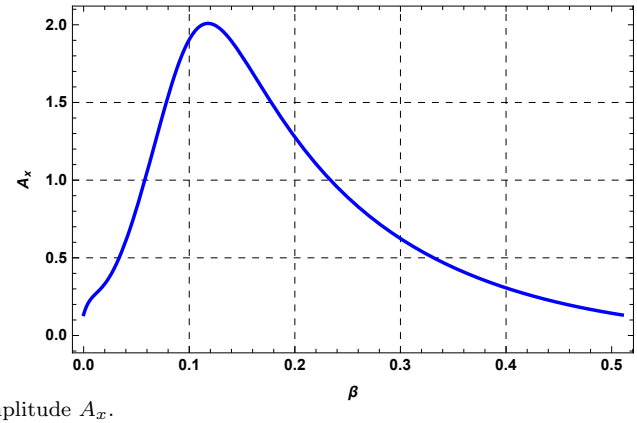

Fig. 5 The effect of β on the amplitude A_x.

However, all the secular terms can not be removed. Additionally, it becomes necessary to specify a phase angle constraint relationships $\psi = \phi + m\pi/2$ where $(m = 1, 3)$. The coefficient l_1 is always negative whereas l_2 is always positive at any value of the β in $[0,\ 1)$. Further, we compute nominal halo orbit, in view of *ISEE–3* mission for which the out–of–plane amplitude $A_z = 110,000$ km and the X–axis amplitude A_x can be found by Eq. 7. Moreover, at different values of β, the amplitude A_x, frequency ω_2 and period T are shown in Table 2. In this context, we investigate graphically, the effect of radiation pressure on the amplitude of in–plane motion in Fig. 5. It is observed that the in–plane amplitude increases in approximately $\beta \in [0, 0.11]$, whereas, it decreases when $\beta > 0.11$ and tends toward 1.

Now, we use a set of algebraic manipulation subroutines developed by [38, 39] to find the third–order periodic solutions under the effect of radiation pressure in the following form

$$\begin{aligned}
x =& a_{21}A_x^2 + a_{22}A_z^2 - A_x\cos\tau_1 \\
&+ (a_{23}A_x^2 - a_{24}A_z^2)\cos 2\tau_1 \\
&+ (a_{31}A_x^3 - a_{32}A_xA_z^2)\cos 3\tau_1 \\
y =& \kappa A_x \sin\tau_1 + (b_{21}A_x^2 - b_{22}A_z^2)\sin 2\tau_1 \\
&+ (b_{31}A_x^3 - b_{32}A_xA_z^2)\sin 3\tau_1 \\
z =& A_z\cos\tau_1 + d_{21}A_xA_z(\cos 2\tau_1 - 3) \\
&+ (d_{32}A_zA_x^2 - d_{31}A_z^3)\cos 3\tau_1
\end{aligned} \tag{8}$$

where $\tau_1 = \lambda\tau + \phi$, while the constants a_{2i} , $(i = 1, 2, 3, 4)$, a_{3j} , b_{2j} , b_{3j} , d_{jj} , $(j = 1, 2)$ and d_{21} are given in Appendix A. Orbit corresponding to the solution (8) is named as halo orbit. Projections of the orbit under the effect of radiation

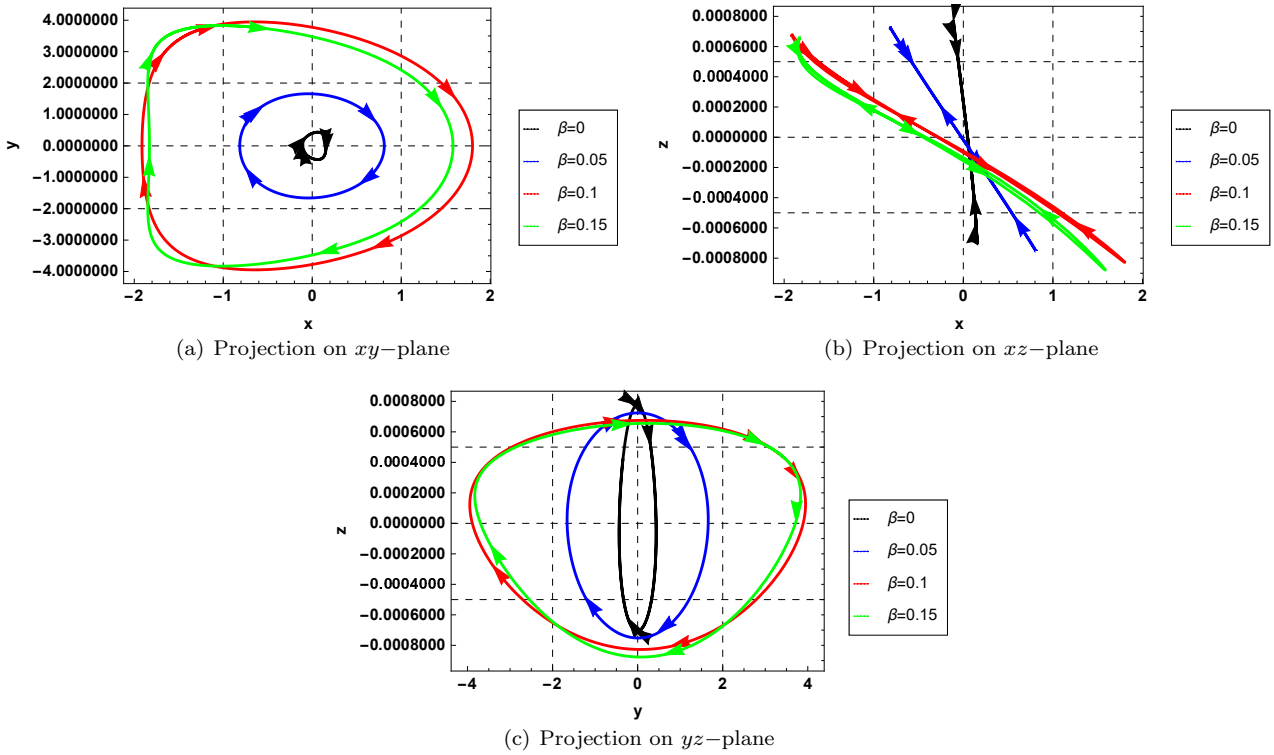

(a) Projection on $xy-$plane

(b) Projection on $xz-$plane

(c) Projection on $yz-$plane

Fig. 6 Halo orbit projections on different plane under the effect of radiation pressure

pressure are shown in Figs. (6) at different values for the parameter β, which represents the perturbation of radiation pressure.

5 Nominal halo orbit by Fourier series

Once the appropriate periodic solutions (8) around the collinear libration point L_1 have been found via Lindstedt–Poincaré technique, we express the solution in terms of Fourier series to realize the nominal halo orbits. The level of approximation is estimated by limits on the accuracy of the analytical technique, which is used to generate the Fourier coefficients. By specifying each of the state variables q_i is to be expressible in the form

$$q_i = \frac{a_0^{(i)}}{2} + \sum_{n\geq 1}\left[A_n^{(i)} + B_n^{(i)}\right], \tag{9}$$

where the terms $A_n^{(i)}$ and $B_n^{(i)}$ are defined by

$$\begin{aligned} A_n^{(i)} &= a_n^{(i)} \cos\left(\frac{2n\pi}{T}t\right), \\ B_n^{(i)} &= b_n^{(i)} \sin\left(\frac{2n\pi}{T}t\right), \end{aligned} \tag{10}$$

and $a_n^{(i)}$ and $b_n^{(i)}$ are the Fourier coefficients, which can be calculated from the following relations

$$\begin{aligned} a_n^{(i)} &= \frac{2}{T}\int_0^T q_i \cos\left(\frac{2n\pi}{T}t\right) dt, \\ b_n^{(i)} &= \frac{2}{T}\int_0^T q_i \sin\left(\frac{2n\pi}{T}t\right) dt, \end{aligned} \tag{11}$$

After utilizing Eqs. (9 , 10 , 11), we accomplish the Fourier series solution.

Integration in these two expressions (11) performed by using Simpson's composite method [40] with a step size chosen as for the error in approximately less than 10^{-10}. The Simpson's composite rule is

$$\begin{aligned} \int_a^b f(x)dx = &\frac{h}{3}\left[f(a) + f(b)\right] \\ &+ \frac{2h}{3}\left[S_1(x_{2j}) + 2S_2(x_{2j-1})\right] \\ &- \frac{b-a}{180}h^4 f^{(4)}(\emptyset), \end{aligned} \tag{12}$$

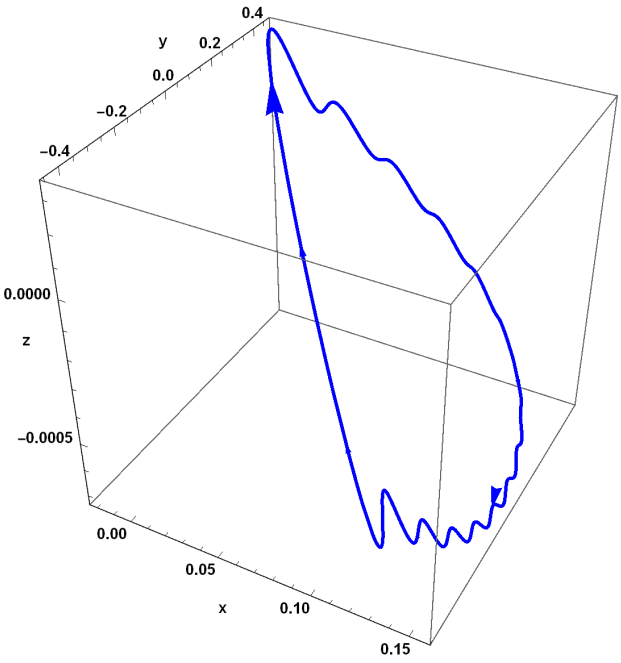

(a) The halo orbit in 3−dimension

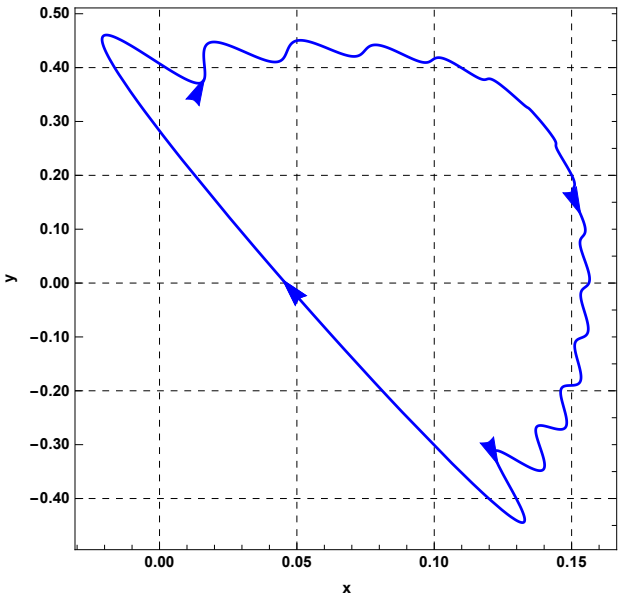

(b) The halo orbit in $XY-$plane

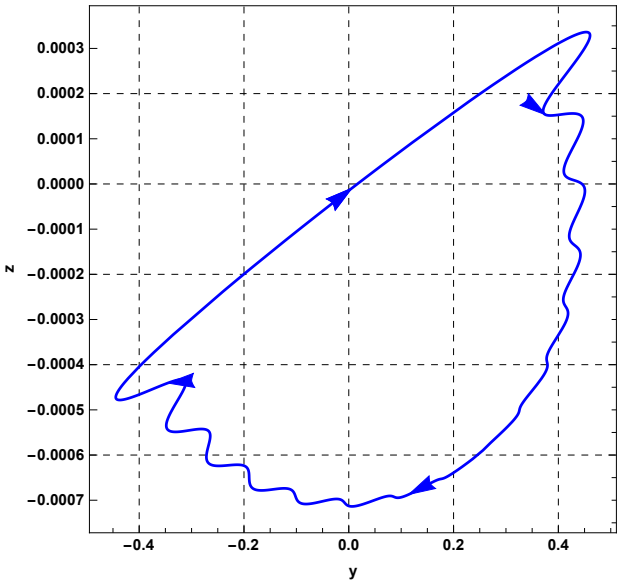

(c) The halo orbit in $YZ-$plane

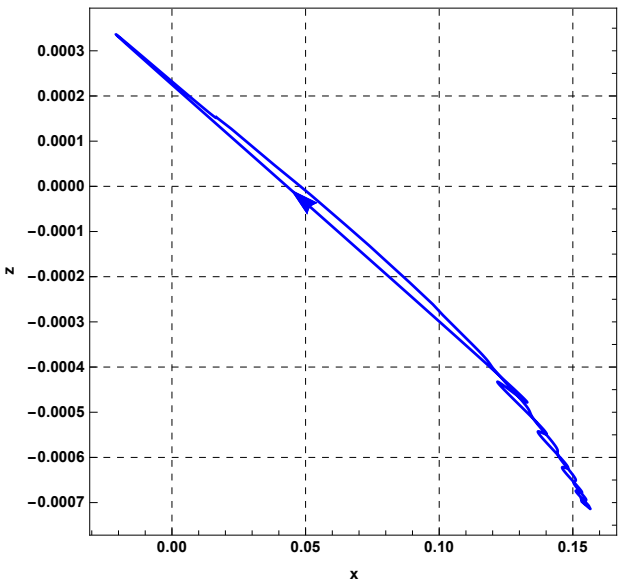

(d) The halo orbit in $XZ-$plane

Fig. 7 Halo orbit in different plane by fourier series.

where

$$S_1(x_{2j}) = \sum_{j=1}^{(m/2)-1} f(x_{2j}),$$
$$S_2(x_{2j-1}) = \sum_{j=1}^{m/2} f(x_{2j-1}), \tag{13}$$

here $f \in C^4[a\,,\,b]$ and $x_j = a + jh$, for each $j = 0, 1, 2 \ldots, n$; there exists $\emptyset \in [a\,,\,b]$. For the halo orbit at $\beta = 0$, the time period $T = 3.05757$. Due to tolerance of error 10^{-10}, we obtained subintervals $m = 592$ and so the step size $h = 0.00516481$. Using this step size and level of tolerance of error, with a help of Eqs. (12 , 13), we found the Fourier coefficients $a_n^{(i)}$ and $b_n^{(i)}$. Further, the state variables which obtained from the third–order approximation using Lindstedt–Poincaré technique, we express in the form of Fourier series.

The configuration of nominal halo orbit by Fourier series is investigated in Fig. 7, where the capture in the $3D$–plane is shown in the Fig. 7(a) and the projections of the orbit in different plane are shown in Figs. [7(b) , 7(c) , 7(d)].

6 Conclusions

In this paper, we have studied the nominal halo orbit in the circular restricted three–body problem within frame of the Sun–Earth system. In this study, we have considered the effect of radiation pressure force by the Sun. The effect of radiation pressure force is discussed for the formation of halo orbits. To ascertain the nominal halo orbits, once we have calculated the appropriate periodic solutions around the collinear libration point L_1 by Lindstedt–Poincaré method, we expressed the solutions as in form of the Fourier series up to $n = 15$. In this context, the Fourier coefficients are found by using the Simpson's composite method. During the formation of the halo orbit using Lindstedt–Poincaré method, we found that the amplitude and period of the halo orbits are perturbed by the radiation pressure force.

The halo orbit shrinks in its amplitude and tends towards the radiating body Sun as value of the β increases. In addition, the time period increases as β increases in interval $\beta \in [0,\ 0.05]$ and then decreased on above values of the β. These findings extend the nature of changes in both in–plane and out–of–plane amplitudes, however we have fixed the out–of–plane amplitude at $110,000\,km$ as that of amplitude *ISEE-3*. The effect of radiation pressure amplifies the effect of the perturbation on the satellite's motion. According to the radiation pressure force, the analysis can be used to design trajectory for spacecraft traveling in more realistic system.

Moreover, by Fourier series expansion, we found the periodic orbit with more analytical expression for the halo orbit. The stable and unstable manifold of the halo orbits and also trajectory transfer would be the interesting topics of further research.

Appendix A

$$
\begin{aligned}
s_1 =& \frac{3c_3}{2D_3}\left[2a_{21}(\kappa^2-2)-a_{23}(\kappa^2+2)-2\kappa b_{21}\right]\\
&-\frac{3c_4}{8D_3}\left(3\kappa^4-8\kappa^2+8\right)\\
s_2 =& \frac{3c_3}{2D_3}\left[2a_{22}(\kappa^2-2)-\zeta a_{24}(\kappa^2+2)\right]\\
&+\frac{3c_3}{2D_3}\left[d_{21}(2-3\zeta)-2\zeta\kappa b_{22}\right]\\
&+\frac{3c_4}{8D_3}\left[(8-4\zeta)-\kappa^2(2+\zeta)\right]
\end{aligned}
$$

$$
\begin{aligned}
a_{21} =& \frac{3c_3(\kappa^2-2)}{4(1+2c_2)}\\
a_{22} =& \frac{3c_3}{4(1+2c_2)}
\end{aligned}
$$

$$
\begin{aligned}
a_{23} =& -\frac{3\lambda c_3}{4\kappa D_1}[3\kappa^3\lambda-6\kappa(\kappa-\lambda)+4]\\
a_{24} =& -\frac{3\lambda c_3}{4\kappa D_1}(2+3\lambda\kappa)\\
a_{31} =& -\frac{9\lambda}{D_2}a_{31}^{11}+\frac{9\lambda^2+1-c_2}{2D_2}a_{31}^{12}\\
a_{32} =& -\frac{9\lambda}{4D_2}a_{32}^{11}-\frac{3(9\lambda^2+1-c_2)}{2D_2}a_{32}^{12}
\end{aligned}
$$

where

$$
\begin{aligned}
a_{31}^{11} =& \left[c_3(\kappa a_{23}-b_{21})+\kappa c_4(1+\frac{1}{4}\kappa^2)\right]\\
a_{31}^{12} =& \left[3c_3(2a_{23}-\kappa b_{21})+c_4\left(2+3\kappa^2\right)\right]\\
a_{32}^{11} =& [4c_3(\kappa a_{24}-b_{22})+\kappa c_4]\\
a_{32}^{12} =& [c_3(\kappa b_{22}+d_{21}-2a_{24})-c_4]
\end{aligned}
$$

$$
\begin{aligned}
b_{21} =& -\frac{3c_3\lambda}{2D_1}(3\lambda\kappa-4)\\
b_{22} =& \frac{3\lambda c_3}{D_1}\\
b_{31} =& \frac{1}{D_2}b_{31}^{11}+\frac{(9\lambda^2+1+2c_2)}{8D_2}b_{31}^{12}\\
b_{32} =& \frac{1}{D_2}b_{32}^{11}+\frac{\left(9\lambda^2+1+2c_2\right)}{8D_2}b_{32}^{12}
\end{aligned}
$$

where

$$
\begin{aligned}
b_{31}^{11} &= \left[3\lambda c_3(\kappa b_{21} - 2a_{23}) - c_4(2+3\kappa^2)\right] \\
b_{31}^{12} &= \left[12c_3(\kappa a_{23} - b_{21}) + 3\kappa c_4(4+\kappa^2)\right] \\
b_{32}^{11} &= \left[3\lambda c_3(\kappa b_{22} + d_{21} - 2a_{24}) - 3c_4\right] \\
b_{32}^{12} &= \left[12c_3(\kappa a_{24} - b_{22}) + 3c_4\kappa\right]
\end{aligned}
$$

$$
\begin{aligned}
d_{21} &= -\frac{c_3}{2\lambda^2} \\
d_{31} &= \frac{3}{64\lambda^2}\left(4c_3a_{24} + c_4\right) \\
d_{32} &= \frac{3}{64\lambda^2}\left[4c_3(a_{23} - d_{21}) + c_4(4+\kappa^2)\right] \\
D_1 &= 16\lambda^4 + 4\lambda^2(c_2 - 2) - 2c_2^2 + c_2 + 1 \\
D_2 &= 81\lambda^4 + 9\lambda^2(c_2 - 2) - 2c_2^2 + c_2 + 1 \\
D_3 &= 2\lambda\left[\lambda\left(1+\kappa^2\right) - 2\kappa\right]
\end{aligned}
$$

Author contributions

All the authors have contributed in an equal way to the research in this paper.

Declaration of competing interests

The authors declare that they have no known competing financial interests or personal relationships that could have appeared to influence the work reported in this paper.

Acknowledgements

The first and second authors is partially supported by Fundación Séneca (Spain), grant 20783/PI/18, and Ministerio de Ciencia, Innovación y Universidades (Spain), grant PGC2018-097198-B-I00.

References

1. E. I. Abouelmagd, A. Mostafa, J. L. Guirao, A first order automated lie transform, International Journal of Bifurcation and Chaos 25 (14) (2015) 1540026.
2. N. Pathak, E. I. Abouelmagd, V. Thomas, On higher order resonant periodic orbits in the photo–gravitational planar restricted three–body problem with oblateness, The Journal of the Astronautical Sciences 66 (4) (2019) 475–505.
3. E. I. Abouelmagd, J. L. G. Guirao, J. Llibre, Periodic orbits for the perturbed planar circular restricted 3-body problem, Discrete Contin. Dyn. Syst.-Ser. B 24 (2019) 1007–1020.
4. S. Abd El-Bar, F. Abd El-Salam, A. Al-Burkani, Computation of the perturbed locations of l1 for all sun–planet rtbp systems with oblate primaries, Results in Physics 15 (2019) 102659.
5. E. E. Zotos, W. Chen, E. I. Abouelmagd, H. Han, Basins of convergence of equilibrium points in the restricted three–body problem with modified gravitational potential, Chaos, Solitons & Fractals 134 (2020) 109704.
6. A. Alshaery, E. I. Abouelmagd, Analysis of the spatial quantized three–body problem, Results in Physics (2020) 103067.
7. A. K. Pal, E. I. Abouelmagd, R. Kishor, Effect of Moon perturbation on the energy curves and equilibrium points in the Sun–Earth–Moon system, New Astronomy 84 (2021) 101505.
8. E. I. Abouelmagd, H. Asiri, M. Sharaf, The effect of oblateness in the perturbed restricted three–body problem, Meccanica 48 (10) (2013) 2479–2490.
9. J. Singh, V. Kalantonis, J. M. Gyegwe, A. Perdiou, Periodic motions around the collinear equilibrium points of the r3bp where the primary is a triaxial rigid body and the secondary is an oblate spheroid, The Astrophysical Journal Supplement Series 227 (2) (2016) 13.
10. E. I. Abouelmagd, F. Alzahrani, J. L. G. Guirao, A. Hobiny, Periodic orbits around the collinear libration points, J. Nonlinear Sci. Appl.(JNSA) 9 (4) (2016) 1716–1727.
11. F. Alzahrani, E. I. Abouelmagd, J. L. G. Guirao, A. Hobiny, On the libration collinear points in the restricted three–body problem, Open Physics 15 (1) (2017) 58–67.
12. H. H. Selim, J. L. Guirao, E. I. Abouelmagd, Libration points in the restricted three-body problem: Euler angles, existence and stability, Discrete & Continuous Dynamical Systems-S 12 (4&5) (2018) 703.
13. N. Pathak, V. Thomas, E. I. Abouelmagd, The perturbed photogravitational restricted three-body problem: Analysis of resonant periodic orbits, Discrete & Continuous Dynamical Systems-S 12 (4&5) (2019) 849–875.
14. R. W. Farquhar, Halo-orbit and lunar-swingby missions of the 1990's, Acta Astronautica 24 (1991) 227–234.
15. T. Wu, X. Pan, M. Xu, Q. Qu, Q. Xia, S. Liu, Parallelly generating halo orbit and its transfer trajectory in the full ephemeris model, Astrophysics and Space Science 364 (1) (2019) 7.
16. M. G. Shirobokov, Libration point orbits and manifolds: design and station-keeping, Keldysh Institute Preprints (90) (2014) 31.

17. K. C. Howell, Three-dimensional, periodic,'halo'orbits, Celestial mechanics 32 (1) (1984) 53–71.
18. A. K. Pal, B. S. Kushvah, Geometry of halo and lissajous orbits in the circular restricted three–body problem with drag forces, Monthly Notices of the Royal Astronomical Society 446 (1) (2015) 959–972.
19. C. Simó, Dynamical systems methods for space missions on a vicinity of collinear libration points, in: Hamiltonian Systems with Three or More Degrees of Freedom, Springer, 1999, pp. 223–241.
20. Y. Zhang, X. Zeng, X. Liu, Study on periodic orbits around the dipole segment model for dumbbell-shaped asteroids, Science China Technological Sciences 61 (6) (2018) 819–829.
21. X. Hou, X. Xin, J. Feng, Genealogy and stability of periodic orbit families around uniformly rotating asteroids, Communications in Nonlinear Science and Numerical Simulation 56 (2018) 93–114.
22. M. Shirobokov, S. Trofimov, M. Ovchinnikov, Survey of station-keeping techniques for libration point orbits, Journal of Guidance, Control, and Dynamics 40 (5) (2017) 1085–1105.
23. Y. Zhang, X. Zeng, F. Zhang, Spacecraft hovering flight in a binary asteroid system by using fuzzy logic control, IEEE Transactions on Aerospace and Electronic Systems 55 (6) (2019) 3246–3258.
24. M. Shirobokov, S. Trofimov, M. Ovchinnikov, On the design of a space telescope orbit around the sun–venus l_2 point, Advances in Space Research 65 (2020) 1591–1606.
25. G. Gómez, A. Jorba, J. Masdemont, C. Simó, Study of the transfer from the earth to a halo orbit around the equilibrium pointl 1, Celestial Mechanics and Dynamical Astronomy 56 (4) (1993) 541–562.
26. M. A. Andreu, C. Simo, Translunar halo orbits in the quasibicircular problem, in: The Dynamics of Small Bodies in the Solar System, Springer, 1999, pp. 309–314.
27. Q. Yingjing, Y. Xiaodong, J. Wuxing, W. Zhang, An improved numerical method for constructing halo/lissajous orbits in a full solar system model, Chinese Journal of Aeronautics 31 (6) (2018) 1362–1374.
28. V. Angelopoulos, The artemis mission, in: The ARTEMIS mission, Springer, 2010, pp. 3–25.
29. T. H. Sweetser, S. B. Broschart, V. Angelopoulos, G. J. Whiffen, D. C. Folta, M.-K. Chung, S. J. Hatch, M. A. Woodard, Artemis mission design, in: The ARTEMIS Mission, Springer, 2012, pp. 61–91.
30. A. J. Abraham, D. B. Spencer, T. J. Hart, Early mission design of transfers to halo orbits via particle swarm optimization, The Journal of the Astronautical Sciences 63 (2) (2016) 81–102.
31. J. Heiligers, C. R. McInnes, J. D. Biggs, M. Ceriotti, Displaced geostationary orbits using hybrid low-thrust propulsion, Acta Astronautica 71 (2012) 51–67.
32. X. Zeng, S. Gong, J. Li, K. T. Alfriend, Solar sail body-fixed hovering over elongated asteroids, Journal of Guidance, Control, and Dynamics 39 (6) (2016) 1223–1231.
33. M. Iñarrea, V. Lanchares, J. F. Palacián, A. I. Pascual, J. P. Salas, P. Yanguas, The effect of j2 on equatorial and halo orbits around a magnetic planet, Chaos, Solitons & Fractals 42 (1) (2009) 155–169.
34. M. Ceccaroni, A. Celletti, G. Pucacco, Halo orbits around the collinear points of the restricted three-body problem, Physica D: Nonlinear Phenomena 317 (2016) 28–42.
35. G. Gómez, J. J. Masdemont, Astrodynamics Network AstroNet-II: The Final Conference, Vol. 44, Springer, 2016.
36. C. Lhotka, A. Celletti, The effect of poynting–robertson drag on the triangular lagrangian points, Icarus 250 (2015) 249–261.
37. R. Farquhar, D. Muhonen, D. Richardson, Mission design for a halo orbiter of the earth, in: Astrodynamics Conference, 1976, p. 810.
38. R. Thurman, P. A. Worfolk, The geometry of halo orbits in the circular restricted three-body problem, University of Minnesota: Geometry Center Research Report GCG95 (1996).
39. R. D. Tiwary, B. S. Kushvah, Computation of halo orbits in the photogravitational sun–earth system with oblateness, Astrophysics and Space Science 357 (1) (2015) 1–16.
40. S. D. Conte, C. De Boor, Elementary numerical analysis: an algorithmic approach, SIAM, 2017.